

Fluorescent N-doped Carbon Dots from Bacterial Cellulose for Highly Sensitive Bacterial Detection

Shunli Li,^a Xin Zhao,^{a,b} Yujie Zhang,^a Honglei Chen,^{a,*} and Yu Liu^{a,*}

Carbon dots have good dispersion capability, strong visible fluorescence, low toxicity, and photo-induced accepting and donating abilities. Carbon dots were obtained from biomass bacterial cellulose (BC) via one-step hydrothermal carbonization. Effects of hydrothermal time and temperature on the microstructure, fluorescence, and excitation wavelength dependent photoluminescence (PL) behavior were explored for the prepared carbon dots. The results showed that the carbon dots obtained directly from the BC (C dots) had small particle sizes (2.0 to 3.0 nm) and green luminescence behavior. Conversely, the N-doped carbon dots (N-C dots) exhibited more uniform and smaller particle sizes (approximately 1.0 nm), strong blue luminescence, acceptable fluorescence lifetime, and good stability in a wide range of pH values (2.0 to 10.0). Thus, carbon dots could serve as a fluorescent material used in high performance optical cellular imaging and highly sensitive bacterial detection.

Keywords: Carbon dots; Bacterial cellulose; Fluorescent; Bacterial detection

Contact information: a: State Key Laboratory of Biobased Material & Green Papermaking, Qilu University of Technology, Shandong Academy of Sciences, Jinan 250353, P.R. China; b: The Key Laboratory of Bio-based Material Science & Technology, Ministry of Education, Northeast Forestry University, Harbin 150040, P.R. China;

* Corresponding authors: chenhonglei_1982@163.com; leoliuyu@163.com

INTRODUCTION

As a novel and fascinating carbon-based material, fluorescent carbon dots with highly sensitive bioimaging, biosensing, and runnable emission are promising alternatives for bacterial detection (Wang *et al.* 2018a; Yang *et al.* 2019). Carbon quantum dots mainly consist of a fraction of nanometer sized carbon core surrounded by amorphous carbon frames, and attract attention because of their chemical stability, dispersibility, low photobleaching, biocompatibility, low cost, and low toxicity (Shih *et al.* 2014; Srinivasan *et al.* 2019). These interesting properties help the new generation of luminescent materials, which are superior to conventionally used fluorescent organic dyes and luminescent inorganic quantum dots. Optimization of properties and modification of chemical activities involves the use of nitrogen (N) as a general dopant element within carbon materials because of its comparable atomic size and participation in strong valence bonds with carbon atoms (Li *et al.* 2015). The presence of additional lone pairs of electrons and the commonly introduced defect sites from N-doping would provide potential active sites and modify the local chemical activities of carbon nanostructures (Zhang *et al.* 2015; Peng *et al.* 2016). Based on the benefits of N-doping in carbon nanostructures, it can be extrapolated that the introduction of N into carbon dots will further enhance their versatile properties, which is extremely important both fundamentally and technologically. Therefore, it is valuable and meaningful to obtain

uniform and ordered N-doped carbon dots (N-C dots) with a highly sensitive performance from low cost raw materials.

The hydrothermal method is the most attractive route for preparing carbon dots because it is a simple, green, and environmentally friendly method (Liu *et al.* 2015; Xu *et al.* 2017). This method involves a chemical reaction in water and an aqueous solution or steam under a certain temperature and pressure. The hydrothermal method allows full use of the carbon resources including recycling (Wang *et al.* 2011; Li *et al.* 2017). Simultaneously, carbon dot doping could be efficiently realized under the hydrothermal environment.

Bacterial cellulose (BC) is an inexpensive, environmentally friendly, abundant, and renewable biomass material. BC can be produced on an industrial scale *via* the microbial fermentation process and has attracted much attention in many fields; however, it has not yet been applied with high value added to the material (Li *et al.* 2018; Ma *et al.* 2019). BC is a naturally occurring nanofibrous biomaterial that exhibits unique physical properties and is amenable to chemical modifications. Long chains of BC molecules could form stable crystalline regions by combining with hydrogen bonds (Huang *et al.* 2019). These characteristics of high purity and good crystallinity are favorable for the formation of uniform structure as well as the improvement of graphitization of carbon materials. Such a characteristic is beneficial to improve fluorescent performance and to broaden the application fields for carbon dots, such as cellular imaging or sensing, drug and gene delivery, and bacterial detection (Wahid *et al.* 2019).

The present study used a one-step hydrothermal route to produce carbon dots using bacterial cellulose in the presence of citric acid. The different properties were tested for the samples prepared at different hydrothermal temperatures and times. This highly efficient method provides a “green” conversion in a “suitable” N doping environment to prepare the functionalized carbons with excellent fluorescence performance. N doping resulted in a higher stability in fluorescence and the sensitive bacterial detection is more effective by introducing C-N polar bond into the prepared carbon dots. This work delivers an environmentally friendly and simple way to achieve high value-added utilization of BC in the fields of cellular imaging and highly-sensitive bacterial detection.

EXPERIMENTAL

Preparation of Fluorescent Carbon Dots (C-dots) and N-C dots

The fluorescent carbon dots were prepared from bacterial cellulose *via* one-step hydrothermal carbonization. The bacterial cellulose (10 g), citric acid (1 mL), urea (0 g or 0.5 g), and deionized water (30 mL) were mixed and sealed into a Teflon-lined autoclave, followed by hydrothermal treatment at different temperatures (220, 230, and 240 °C) for different times (4 h, 6 h, and 8 h). The obtained liquid product was centrifuged (18,000 ×g, 20 min) and the resultant supernatant containing luminescent C-dots was dialyzed with a 2000 NWCO dialysis tube against deionized water for 24 h. The prepared samples donated as C-dots-X-Y and N-C-dots-X-Y (X is hydrothermal temperature, Y is hydrothermal time, N is with urea), respectively.

Characterization

The transmission electron microscopy (TEM) images of the prepared carbon dots were obtained on a JEOL 2011 apparatus (Shoshima, Japan) operated at 200 kV. The

powder X-ray diffraction (XRD) patterns were measured using a Bruker D4 powder X-ray diffractometer (Karlsruhe, Germany) with Cu K α radiation at 40 kV and 40 mA. The Raman measurement was performed using a microRaman and reflex spectrometer (Renishaw, Gloucestershire, England) (laser wavelength: 532 nm). Chemical properties of the samples were evaluated by X-ray photoelectron spectroscopy (XPS) on an ESCALAB 250 apparatus by Thermo Fisher (Massachusetts, USA) with Al K α radiation. Optical adsorption spectra (UV-vis) of the carbon dots were measured on a UV-3600 (Shimadzu, Kyoto, Japan) spectrometer. A FL-7000 fluorescence spectrometer (Hitachi, Hitachi City, Japan) was used to follow the fluorescence spectra of the carbon dots. Fluorescent imaging was tested with confocal laser scanning microscopy using the Leica DMI8 (Wetzlar, Germany) under different wave lengths. Atomic force microscopy (AFM) was employed to observe carbon dots using a Nanoscope III (Veeco Co. Ltd., Oyster City, NY, USA).

Yeast Cell Detection

Yeast cells (0.05 g) were added into 5 mL of different carbon dots solution (C-dots-230-6 and N-C-dots-230-6) by a sterile operation, respectively. Then they were mixed and activated at 30 °C for 24 h. The labeled cells with fluorescence were separated and collected by centrifugation. The collected cell containing conjugate was thoroughly washed and re-suspended using ultrapure water for fluorescence detection by a Leica DMI3000 inverted fluorescence microscope *via* DAPI, GEP, and Rhod filters.

RESULTS AND DISCUSSION

Overview

Figure 1 provides a schematic diagram for the preparation of C-dots and N-C dots *via* hydrothermal carbonization from bacterial cellulose in the presence of citric acid. The products were separated to solid and liquid, and the obtained aqueous extract contained fluorescent C-dots and N-C dots. The different carbon dots exhibited different size and fluorescence properties.

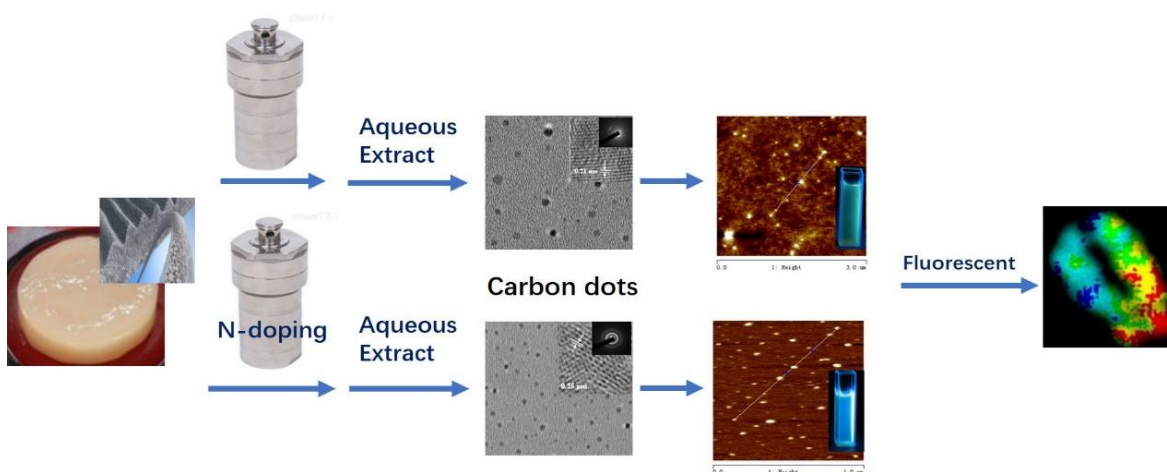


Fig. 1. A schematic diagram of the preparation route of the C-dots and N-C dots

Electron Microscopy

The morphologies of C-dots at different hydrothermal times and temperatures were characterized by transmission electron microscopy (Fig. 2a-e). All the C-dots have a quasi-spherical shape with different diameters in the range of 1 nm to 5 nm.

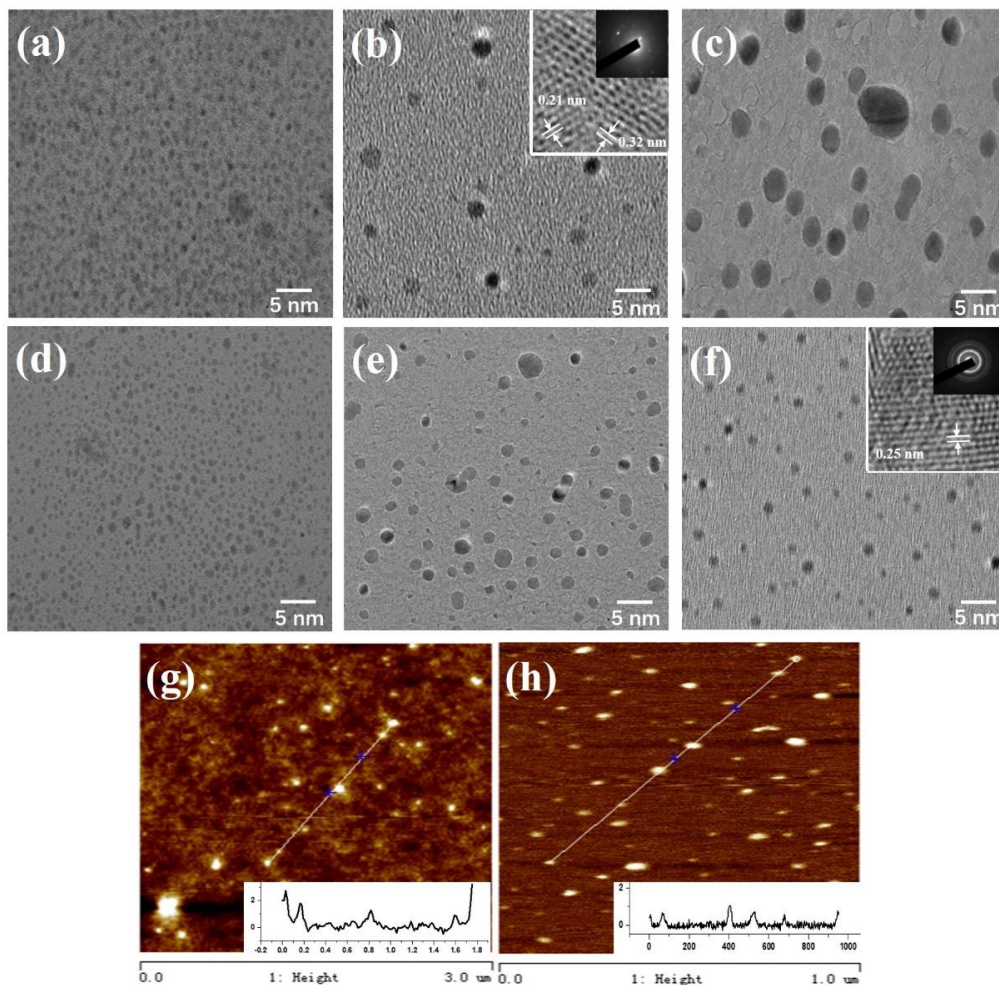


Fig. 2. TEM (a: C-dots-230-4, b: C-dots-230-6, c: C-dots-230-8, d: C-dots-220-6, e: C-dots-240-6, f: N-C-dots-230-6) and AFM images (g: C-dots-230-6, h: N-C-dots-230-6) of the carbon dots from different hydrothermal conditions.

The diameters increased and distribution of C-dots became more uniform with hydrothermal time increased from 4 h to 8 h, respectively (Fig. 2a-c). The similar tendency occurred with the hydrothermal temperature increased from 220 to 240 °C (Fig. 2d-f). The phenomenon may be attributed to an easier aggregation of C-dots at higher hydrothermal temperatures and during a longer time (Zheng *et al.* 2019). The results indicate that the C-dots-230-6 displays uniform spherical size (approximately 2.0 to 3.0 nm) with homogeneous distribution. Additionally, more uniform and smaller size (approximately 1.0 to 2.0 nm) of the N-C dots were obtained by the facile N-doping method. High resolution TEM images illustrate crystallinity of the prepared C-dots and N-C dots, as shown in the inset of Fig. 1b, f. The lattice parameter of C-dots is *ca.* 0.21 and 0.32 nm, corresponding to the lattice plane (102), (002) of graphite. However, the lattice parameter of N-C dots is 0.25 nm. The mismatch of lattice parameters could be due to the presence of nitrogen and oxygen, which have also been observed in other

nitrogen or oxygen rich carbon dots (Li *et al.* 2012, 2013; Tang *et al.* 2012; Habiba *et al.* 2013). The AFM images (Fig. 2g, h) further confirmed the quasi-spherical shape and good disbursement of the prepared C-dots and N-C dots. The topographic heights of N-C-dots-230-6 were mostly between 1 to 2 nm and more uniform than that of C-Dots, which is consistent with the results of TEM analysis.

X-Ray Photoelectron Spectroscopy

The structures of the prepared carbon dots were further investigated by XRD, Raman, and XPS. The XRD pattern of the C-dots showed one reflex at approximately 23° that can be indexed to the (002) reflections of the graphitic carbon (Fig. 3a) (Zhao *et al.* 2015).

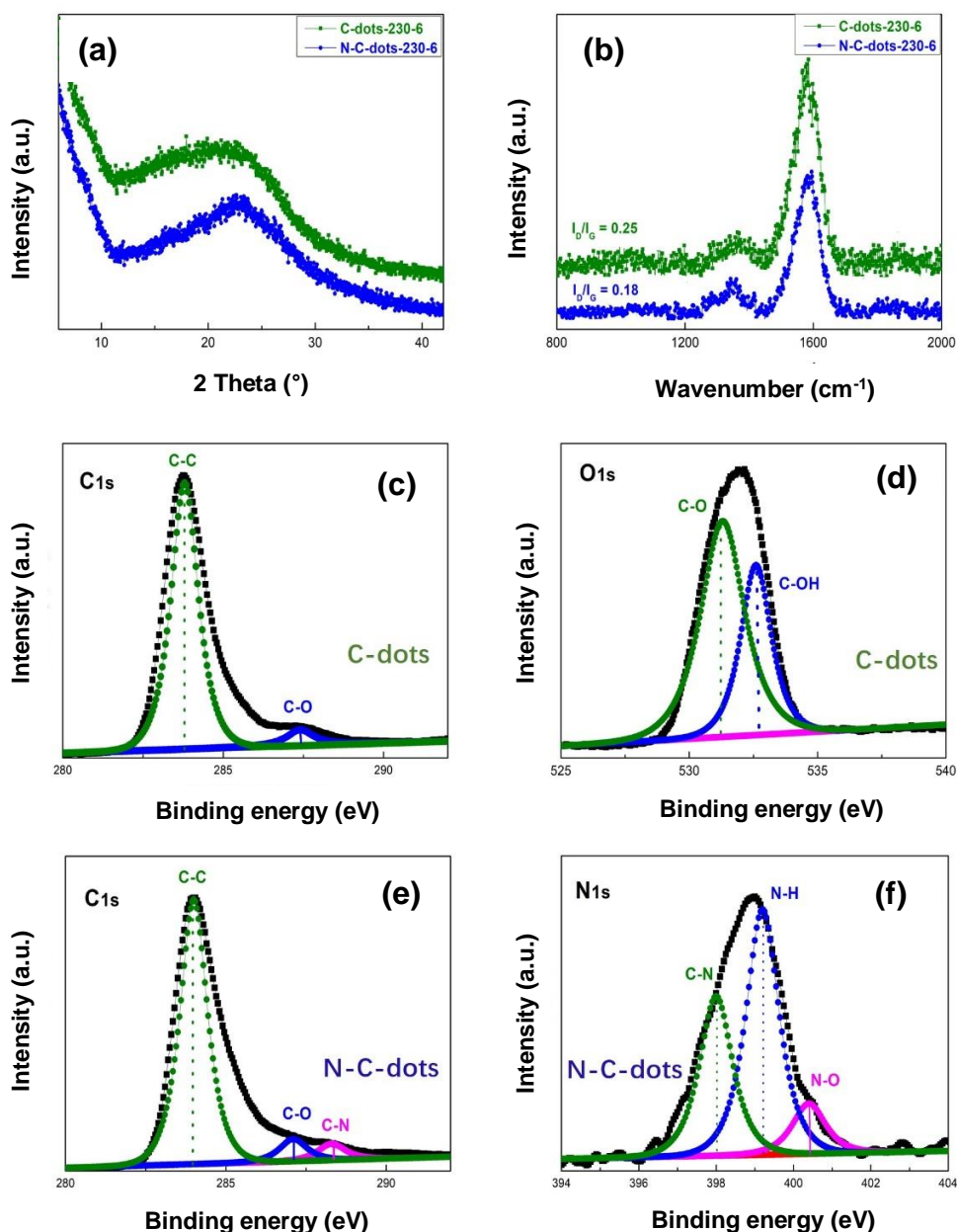


Fig. 3. XRD (a) Raman (b) and XPS (c-f) images of the C-dots and N-C dots

The peaks of N-C dots gradually sharpening indicate a high degree of crystallinity and the graphitization of the N-C dots, which may be due to the presence of N functional groups improved the local chemical activities and graphitized structure of carbon dots. The Raman spectrum of the samples showed two peaks: the peak at 1335 cm^{-1} (D band) reflects the characteristic feature of disordered graphite or crystal defects (C-C), while the G band at 1597 cm^{-1} corresponds to graphitic carbon (Fig. 3b) (Ma *et al.* 2017). Moreover, the ratio of I_D/I_G decreased from 0.25 to 0.18 as a result of the N-doping process, suggesting the formation of an excellent degree of graphitization for N-C dots, which is in agreement with the XRD results. The nature of the carbon, oxygen, and nitrogen species on the surface of the C-dots and N-C dots were explored by XPS technology in Fig. 3c-f. In the C1s spectrum of C-dots (Fig. 3c), peaks for graphitic carbon (C-C, C-H) and ester or ether (C-O) were observed at a binding energy of 284.1 eV and 284.8 eV, respectively (Gong *et al.* 2019). Each O1s spectrum was resolved into two individual component peaks, namely: (1) hydroxyl groups (C-OH, BE = 533.02 eV), (2) ester or ether (C-O, BE = 531.3 eV) (Fig. 3d) (Arul and Sethuraman 2018). The results exhibit abundant carbon-oxygen functional groups (C-C, C-H, C-O and C-OH) on the surface of the samples because of formation of the carbon dots. However, N-C dots showed that the additional peak at 288.4 eV for the C 1s spectrum belongs to C-N coordination (Wang *et al.* 2018b), revealing the recovery of covalent bonding and the existence of nitrogen atoms in carbon graphene layers (Fig. 3e). The detailed information about the nitrogen doping groups can be found in the N 1s spectrum (Fig. 3f). The N 1s spectrum can be deconvoluted into three peaks located at 397.9, 399.3, and 400.4 eV, which could be assigned to C-N, N-H, and N-O (Deng *et al.* 2016; Kim *et al.* 2018; Yang *et al.* 2018), respectively. The results indicate that N-C dots with surface functionalization of O or N-containing groups were successfully obtained. In addition, the optimized performance is attributed to N functional groups, which could provide active sites and modify the local chemical activities of carbon nanostructures by: the presence of the additional lone pairs of electrons and the commonly introduced defect sites from N doping (Peng *et al.* 2016).

Optical Properties

The optical properties of the prepared C-dots and N-C dots were investigated to identify the contributions of the N-doping to fluorescence. Although the color of the C-dots and N-C dots were similar in optical views, distinct differences of absorption spectra were observed. The absorption peak of the C-dots was around 275 nm, while N-C dots showed an absorption feature around 275 nm and 320 nm in UV-vis absorption spectrum (Fig. 4a, d). These shoulder peaks correspond to p-p* transition of C=C bonds and n-p* transition of C=O bonds, respectively (Xu *et al.* 2016). As shown in UV-visible absorption and photoluminescence emission spectra (Fig. 4b, e), the maximum emission peak wavelengths of the C-dots and N-C dots were at approximately 440 nm and 469 nm. Those wavelengths correspond to 380 nm and 400 nm excitation, and appeared green and strong in blue luminescence behavior, respectively. This is a typical excitation-wavelength-dependent photoluminescence emission for C-dots, and the N-C dots sample showed stronger intensity in Fig. 4e. These results indicate that the N-doped process not only plays key roles in the emission wavelength of the carbon dots, but also contributes to fluorescence intensity due to N functional groups providing active sites for carbon dots. Additionally, all the prepared carbon dots exhibited acceptable fluorescence lifetime and better stability in a wide range of pH values (pH 2.0 to 10.0) (Fig. 4c, f), and N-C dots

were relatively more stable (Fig. 4f). The results indicate that N-doping is very effective in modifying surface state and achieving brighter fluorescence emissions (Zhu *et al.* 2012).

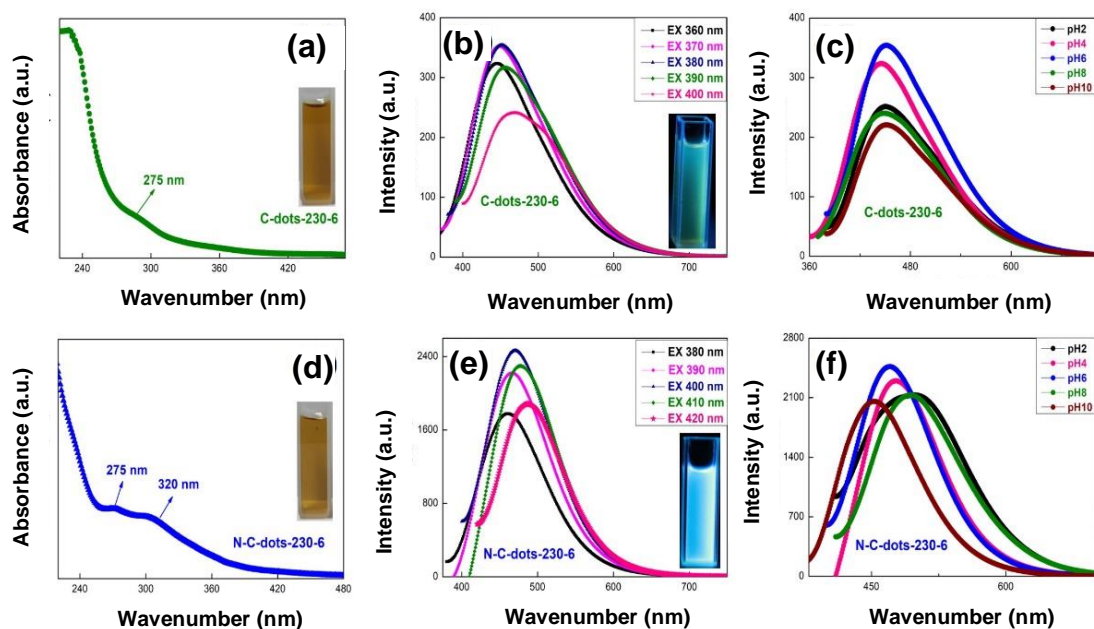


Fig. 4. Optical properties of different carbon dots: Absorption spectra of the C-dots (a) and N-C dots (d) (inset: UV radiation (left) and photograph under day light (right)); Fluorescence spectra with different excitations ranges from 360 nm to 400 nm of the C-dots (b) and N-C dots (e) (inset: curves of Em changes with Ex (left) and photograph under UV light (right)); fluorescence spectra with different pH ranges from 2 to 10 of the C-dots (c) and N-C dots (f).

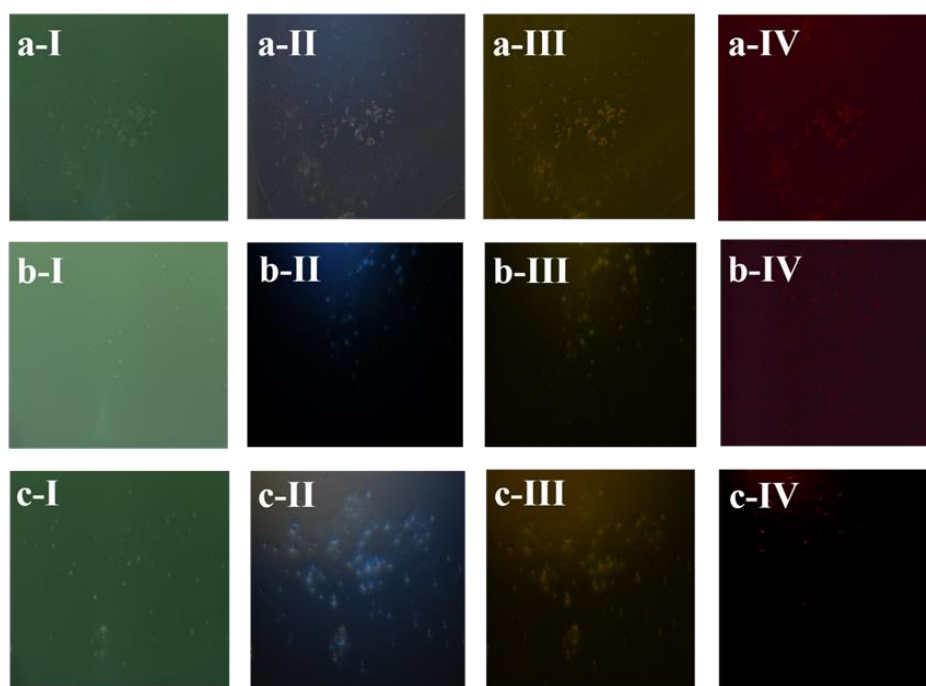


Fig. 5. Bright field (I), DAPI (II), GEP (III), and Rhod filters (IV) fluorescence images of yeast cells (a), labeled yeast cells with C-dots (b), and N-C dots (c), respectively.

The yeast cells (Fig. 5a) and fluorescent labeled of yeast cells with C-dots (Fig. 5b) or N-C dots (Fig. 5c) were evaluated through confocal fluorescence microscopic imaging under DAPI (Fig. 5II), GEP (Fig. 5III), and Rhod filters (Fig. 5IV). The yeast cells showed no light effect in different filters, but it is obvious that the labeled cell displayed different fluorescence effects in the field of view, and the cells with N-C dots showed slightly stronger fluorescence effects under Rhod filters (Fig. 5-cIV). This may be attributed to the high-performance fluorescence intensity of N groups (Wang *et al.* 2018c). These performances demonstrate that the suitability of carbon dots serving as a potential alternative fluorescence probe for cell imaging can provide fluorescence further as sensitizers for bacterial detection (Feng and Qian 2017).

CONCLUSIONS

1. Two types of luminescent carbon dots were prepared by using bacterial cellulose as a carbon source, with and without urea as nitrogen sources at the citric acid condition *via* hydrothermal reaction. The investigation on the structure, optical, photoluminescence properties, and pH-sensitivity of the prepared carbon dots with and without the N-doped process illustrates that nitrogen source plays a key role for optimizing performance by providing active sites and modifying the local chemical activities of carbon nanostructures from N functional groups.
2. The carbon dots without the N-doped process display uniform spherical sizes (approximately 2.0 to 3.0 nm) with homogeneous distribution and exhibit green luminescent light. N-C dots display more uniform, smaller size dots (approximately 1.0 to 2.0 nm) that display stronger blue luminescent light. These results indicate that N-doped not only plays key roles in graphitized structure and the emission wavelength of the carbon dots, but also contributes to fluorescence intensity.
3. Importantly, the N-C dots achieve brighter fluorescence emissions, acceptable fluorescence lifetime, and better stability in a wide range of pH values (pH 2.0 to 10.0), which can provide a fluorescent agent as sensitizers for bacterial detection. In other words, this strategy provides a novel and efficient way for utilization of biomass resources by converting them to value-added materials.

ACKNOWLEDGMENTS

The present work was financially supported by the National Natural Science Foundation of China (Grant Nos. 31800499, 31600472, 31770626), the Key Laboratory of Bio-based Material Science & Technology (Northeast Forestry University), Ministry of Education (grant no. SWZ-MS201910).

REFERENCES CITED

- Arul, V., and Sethuraman, M. G. (2018). "Facile green synthesis of fluorescent N-doped carbon dots from *Actinidia deliciosa* and their catalytic activity and cytotoxicity applications," *Opt. Mater.* 78, 181-190. DOI: 10.1016/j.optmat.2018.02.029

- Deng, Y., Xie, Y., Zou, K.X., and Ji, X.L. (2016). "Review on recent advances in nitrogen-doped carbons: preparations and applications in supercapacitors," *J Mater. Chem. A* 4 (4), 1144-1173. DOI: 10.1039/C5TA08620E
- Feng, H., and Qian, Z. (2017). "Functional carbon quantum dots: a versatile platform for chemosensing and biosensing," *Chem. Rec.* 17, 1-16. DOI: 10.1002/tcr.201700055
- Gong, P., Sun, L., Wang, F., Liu, X., Yan, Z., Wang, M., Zhang, L., Tian, Z., Liu, Z., and You, J. (2019). "Highly fluorescent N-doped carbon dots with two-photon emission for ultrasensitive detection of tumor marker and visual monitor anticancer drug loading and delivery," *Chem. Eng. J.* 356, 994-1002. DOI: 10.1016/j.cej.2018.09.100
- Habiba, K., Makarov, V. I., Avalos, J., Guinel, M. J. F., Weiner, B. R., and Morell, G. (2013). "Luminescent graphene quantum dots fabricated by pulsed laser synthesis," *Carbon* 64, 341-350. DOI: 10.1016/j.carbon.2013.07.084
- Huang, R., Cao, C., Liu, J., Sun, D., and Song, W. (2019). "N-doped carbon nanofibers derived from bacterial cellulose as an excellent metal-free catalyst for selective oxidation of arylalkanes," *Chem. Commun.* 55(13), 1935-1938. DOI: 10.1039/C9CC00185A.
- Kim, D. K., Kim, N. D., Park, S. K., Seong, K., Hwang, M., You, N. H., and Piao, Y.Z. (2018). "Nitrogen doped carbon derived from polyimide/multiwall carbon nanotube composites for high performance flexible all-solid-state supercapacitors," *J. Power. Sources.* 380 (15), 55-63. DOI: 10.1016/j.jpowsour.2018.01.069
- Li, H., Kong, W., Liu, J., Liu, N., Huang, H., Liu, Y., and Kang, Z. (2015). "Fluorescent N-doped carbon dots for both cellular imaging and highly-sensitive catechol detection," *Carbon* 91, 66-75. DOI: 10.1016/j.carbon.2015.04.032
- Li, L., Wu, G., Yang, G., Peng, J., Zhao, J., and Zhu, J.J. (2013). "Focusing on luminescent graphene quantum dots: current status and future perspectives," *Nanoscale* 5, 4015-4039. DOI: 10.1039/c3nr33849e
- Li, Y., Liu, Y., Wang, M., Xu, X., Lu, T., Sun, C.Q., and Pan, L. (2018). "Phosphorus-doped 3D carbon nanofiber aerogels derived from bacterial-cellulose for highly-efficient capacitive deionization," *Carbon* 130, 377-383. DOI: 10.1016/j.carbon.2018.01.035
- Li, Y., Zhao, Y., Cheng, H., Hu, Y., Shi, G., and Dai, L. (2012). "Nitrogen-doped graphene quantum dots with oxygen-rich functional groups," *J. Am. Chem. Soc.* 134, 15-18. DOI: 10.1021/ja206030c
- Li, Y., Zhou, Q., Yuan, Y., and Wu, Y. (2017). "Hydrothermal synthesis of fluorescent carbon dots from sodium citrate and polyacrylamide and their highly selective detection of lead and pyrophosphate," *Carbon* 115, 550-560. DOI: 10.1016/j.carbon.2017.01.035
- Liu, R. L., Zhang, J., Gao, M. P., Li, Z. L., Chen, J. Y., Wu, D. Q., and Liu, P. (2015). "A facile microwave-hydrothermal approach towards highly photoluminescent carbon dots from goose feathers," *RSC Adv.* 5, 4428-4433. DOI: 10.1039/c4ra12077a
- Ma, X., Lou, Y., Chen, X.B., Shi, Z., and Xu, Y. (2019). "Multifunctional flexible composite aerogels constructed through in-situ growth of metal-organic framework nanoparticles on bacterial cellulose," *Chem. Eng. J.* 356, 227-235. DOI: 10.1016/j.cej.2018.09.034
- Ma, X., Zhou, Y., Chen, M., and Wu, L. (2017). "Synthesis of olive-like nitrogen-doped carbon with embedded Ge nanoparticles for ultrahigh stable lithium battery anodes," *Small* 13(20), 1700403. DOI: 10.1002/sml.201700403

- Peng, H., Li, Y., Jiang, C., Luo, C., Qi, R., Huang, R., Duan, C. G., and Seidic, J. T. (2016). "Tuning the properties of luminescent nitrogen-doped carbon dots by reaction precursors," *Carbon* 100, 386-394. DOI: 10.1016/j.carbon.2016.01.029
- Shih, Y. W., Tseng, G. W., Hsieh, C. Y., Li, Y. Y., and Sakoda, A. (2014). "Graphene quantum dots derived from platelet graphite nanofibers by liquid-phase exfoliation," *Acta. Mater.* 78, 314-319. DOI: 10.1016/j.actamat.2014.06.027
- Srinivasan, V., Jhonsi, M. A., Kathiravan, A., and Ashokkumar, M. (2019). "Fuel waste to fluorescent carbon dots and its multifarious applications," *Sensor. Actuat. B-Chem.* 282, 972-983. DOI: 10.1016/j.snb.2018.11.144
- Tang, L., Ji, R., Cao, X., Lin, J., Jiang, H., and Li, X. (2012). "Deep ultraviolet photoluminescence of water-soluble self-passivated graphene quantum dots," *ACS Nano* 6, 5102-5110. DOI: 10.1021/nn300760g
- Wahid, F., Hu, X. H., Chu, L. Q., Jia, S. R., Xie, Y. Y., and Zhong, C. (2019). "Development of bacterial cellulose/chitosan based semi-interpenetrating hydrogels with improved mechanical and antibacterial properties," *Int. J. of Biol. Macromol.* 122, 380-387. DOI: 10.1016/j.ijbiomac.2018.10.105
- Wang, C., Hu, T. T., Thomas, T., Song, S. L., Wen, Z. Q., Wang, C. X., Song, Q. J., and Yang, M. H. (2018a). "Surface state-controlled C-dot/C-dot based dual-emission fluorescent nanothermometers for intra-cellular thermometry," *Nanoscale* 10(46), 21809-21817. DOI: 10.1039/C8NR07445C
- Wang, J. G., Liu, H., Sun, H., Hua, W., Wang, H., Liu, X., and Wei, B. (2018b). "One-pot synthesis of nitrogen-doped ordered mesoporous carbon spheres for high-rate and long-cycle life supercapacitors," *Carbon* 127, 85-92. DOI: 10.1016/j.carbon.2017.10.084
- Wang, J. L., Teng, J. Y., Jia, T., and Shu, Y. (2018c). "Detection of yeast of *Saccharomyces cerevisiae* with ionic liquid mediated," *Talanta* 178, 818-824. DOI: 10.1016/j.talanta.2017.10.029
- Wang, Q., Zheng, H., Long, Y., Zhang, L., Gao, M., and Bai, W. (2011). "Microwave-hydrothermal synthesis of fluorescence carbon dots from graphite oxide," *Carbon* 49, 3134-3140. DOI: 10.1016/j.carbon.2011.03.041
- Xu, M., Huang, Q., Sun, R., and Wang, X. (2016). "Simultaneously obtaining fluorescent carbon dots and porous active carbon for supercapacitors from biomass," *RSC Adv.* 6(91), 88674-88682. DOI: 10.1039/C6RA18725K
- Xu, Y. H., Li, D., Liu, M. L., Niu, F. S., Liu, J. Q., and Wang, E. K. (2017). "Enhanced-quantum yield sulfur/nitrogen co-doped fluorescent carbon nanodots produced from biomass *Enteromorpha prolifera*: Synthesis, posttreatment, applications and mechanism study," *Sci. Rep-UK.* 7(1), 4499-4510. DOI:10.1038/s41598-017-04754-x
- Yang, J. J., Gao, G., Zhang, X. D., Ma, Y. H., and Wu, F. G. (2019). "One-step synthesis of carbon dots with bacterial contact-enhanced fluorescence emission: Fast Gram-type identification and selective Gram-positive bacterial inactivation," *Carbon* 146, 827-839. DOI: 10.1016/j.carbon.2019.02.040
- Yang, W., Hou, L., Xu, X., Li, Z., Ma, X., Yang, F., and Li, Y. (2018). "Carbon nitride template-directed fabrication of nitrogen-rich porous graphene-like carbon for high performance supercapacitors," *Carbon* 130, 325-332. DOI: 10.1016/j.carbon.2018.01.032
- Zhang, J. J., Wang, Z. B., Li, C., Zhao, L., Liu, J., Zhang, L. M., and Gu, D. M. (2015). "Multiwall-carbon nanotube modified by N-doped carbon quantum dots as Pt catalyst

support for methanol electrooxidation,” *J. Power. Sources.* 289, 63-70. DOI: 10.1016/j.jpowsour.2015.04.150

Zhao, X., Li, W., and Liu, S. X. (2015). “Facile fabrication of hollow and honeycomb-like carbon spheres from liquefied larch sawdust *via* ultrasonic spray pyrolysis,” *Mater. Lett.* 157, 135-138. DOI: 10.1016/j.matlet.2015.05.057

Zheng, X., Ding, G., Wang, H., Cui, G., and Zhang, P. (2019). “One-step hydrothermal synthesis of carbon dots-polymer composites with solid-state photoluminescence,” *Mater. Lett.* 238, 22-25. DOI: 10.1016/j.matlet.2018.11.147

Zhu, C., Zhai, J., and Dong, S. (2012). “Bifunctional fluorescent carbon nanodots: Green synthesis via soymilk and application as metal-free electrocatalysts for oxygen reduction,” *Chem. Commun.* 48, 9367-9369. DOI: 10.1039/c2cc33844k

Article submitted: September 11, 2019; Peer review completed: October 26, 2019;
Revised version received: October 31, 2019; Accepted: November 1, 2019; Published:
November 8, 2019.

DOI: 10.15376/biores.15.1.78-88